WARSAW UNIVERSITY OF TECHNOLOGY Index 351733
FACULTY OF CIVIL ENGINEERING
COMMITTEE FOR CIVIL AND WATER ENGINEERING
POLISH ACADEMY OF SCIENCES ISSN 1230-2945
DOI: 10.24425/ace.2024.149867
ARCHIVES OF CIVIL ENGINEERING
Vol. LXX ISSUE 2 2024
pp. 343 –355
© 2024. Andrzej Helowicz.
This is an open-access article distributed under the terms of the Creative Commons Attribution-NonCommercial-NoDerivatives License (CC BY-NC-ND 4.0, https://creativecommons.org/licenses/by-nc-nd/4.0/), which permits use, distribution, and reproduction in any medium, provided that the Article is properly cited, the use is non-commercial, and no modifications or adaptations are made.

Research paper

Modelling of foundation stiffness beneath intermediate support of 178 m long integral viaduct

Andrzej Helowicz[1]

Abstract: The paper presents three methods of modelling of foundation stiffness beneath intermediate support of a 178 m long integral box girder viaduct and its impact on the values and distribution of displacements and internal forces in the pier of this support. The pier support is made of cast in situ reinforced concrete of strength class C50/60. For the analysis, three models were built in Abaqus FEA software. The first model A3D in Fig. 1 represents a complex three-dimensional model. The second L2D and the third H2D model shown in Fig. 2 represent simple two-dimensional models. The stiffness of the subgrade beneath the structure in the second and third model was modelled as spring constants calculated based on the equations given in the reference [8] model L2D and [10] model H2D. The middle range value of Young's modulus for sand and gravel was used to calculate the subgrade stiffness parameters. In all models, a horizontal displacement in the Y direction of value 20 mm and a vertical force of value 18200 kN were applied to the top of the pier support. The horizontal displacement was caused by the thermal longitudinal expansion of the six-span viaduct deck and the braking force. The vertical force was caused by the dead, superimposed, and live loads acting on the viaduct deck. Finally, the values and distributions of displacements and internal forces in the pier support from the complex model were compared with the values in two simple models. The author focuses on the method of modelling of foundation stiffness of the pier support and its impact on the values of displacements and internal forces in the pier support. A similar structure analysed in this paper was design-checked by the author in Ireland [4].

Keywords: design, integral viaduct, intermediate support, foundation stiffness

[1]PhD., Eng., Wrocław University of Science and Technology, Faculty of Civil Engineering, Na Grobli 15, 50-421 Wrocław, Poland, e-mail: andrzej.helowicz@pwr.edu.pl, ORCID: 0000-0001-9527-1281

1. Introduction

The paper presents three methods of modelling of the foundation stiffness beneath intermediate support of a 178 m long integral box girder viaduct and its impact on the values and distribution of displacements and internal forces in the pier of this support. The pier support is monolithically connected to its footing foundation and the box viaduct girder. An integral viaduct can be defined as a viaduct whose spans are monolithically connected with the intermediate supports and abutment walls and whose structure interacts with the surrounding soil due to thermal effects and permanent and variable vehicle and pedestrian traffic loads. Such elements as viaduct bearings, mechanical expansion joints and approach slabs are not required in this case, whereby the construction and maintenance of integral viaduct is less expensive. The analysed pier support and the footing foundation is made of cast in situ reinforced concrete of strength class C50/60. The concrete tangent modulus of elasticity used in the analysis has a value of 37 GPa [14]. The selected support is the last of five intermediate supports carrying the integral six spans viaduct. The Young's modulus E of the subgrade beneath the structure selected in the analysis applies to granular materials for example, dense sand and gravel [10]. Middle range value of Young's modulus for dense sand and gravel was used in the analysis. For the purpose of the analysis, three numerical models were built in the Abaqus FEA software [13]. The first A3D model shown in Fig. 1 represents a complex three-dimensional model.

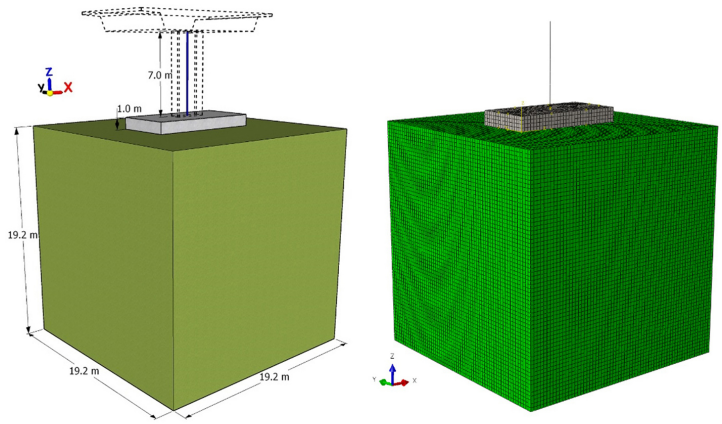

Fig. 1. Numerical complex model

The second L2D and third H2D model shown in Fig. 2 are simplified two-dimensional models.

The stiffness of footing in the latter two models was replaced by the rocking, vertical and horizontal springs. The stiffnesses of these springs were calculated using the equations given in publication [8] for the L2D model and publication [10] for the H2D model. The equations for calculating the springs stiffness for a rectangular footing given by Barkan [11]

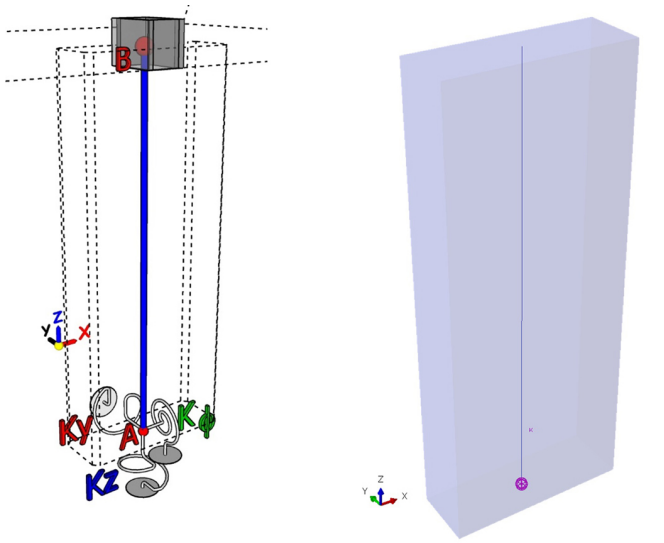

Model sketch *Model in Abaqus FEA software [13]*

Fig. 2. Numerical simple model: L2D, H2D

and Gorbunov–Possadov [12], used in the models, were derived from the theory for an elastic half space. Since the 1960s, these equations have been used in the design of concrete foundations for heavy industrial machinery that induces additional dynamic loads [11]. These equations are also used in the design of integral bridges [10]. Finally, the results of static calculations, such as displacements and internal forces in the pier support from the complex three-dimensional model were compared with two simple two-dimensional models.

The design and construction of a similar structure is described more thoroughly in the publication [4]. Other types of integral bridges and viaducts, both single-span and multi-span ones, arch bridges and box bridges, are described in the papers [1–7]. It should be noted that the implementation of integral viaducts and bridges on the M18 motorway from Limerick to Galway in Ireland, in which the author was involved in the design, contributed to a significant reduction in the time and cost of the construction of the motorway.

2. Description of analysed element

The selected pier support is the last of five intermediate supports supporting a six-span viaduct with a deck length of 178 m. The main dimensions of the pier support and the footing foundation are shown in Fig. 3.

The footing foundation and the pier support are made of C50/60 strength class reinforced concrete cast in-situ. The pier support is monolithically connected to the footing foundation and to the viaduct deck. In the analysis, it was assumed that the structure rests on granular material, for example dense sand and gravel of overall depth equal to 19.2 m. The

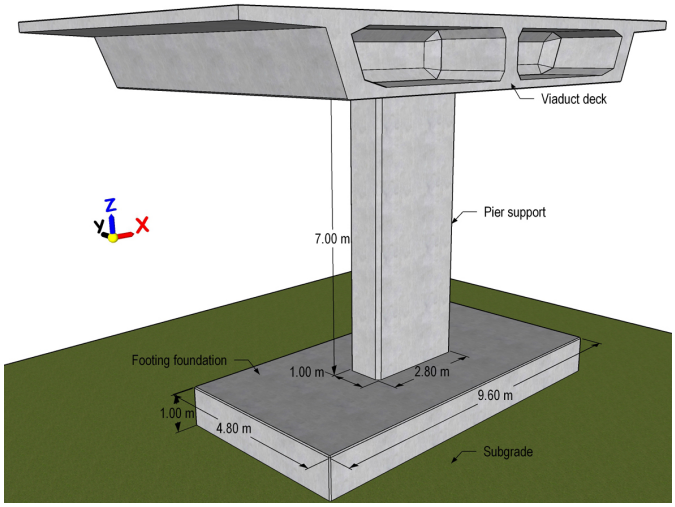

Fig. 3. Axonometric view of the intermediate support

elastic properties of the selected materials were taken from the publication [10]. It should be emphasized that prior to design calculations that take subgrade stiffness into account, the proper soil parameters for the subgrade under the structure must be determined. On the basis of such data, the designer can build a numerical model of the structure founded on the specific subgrade stiffness. Therefore, close cooperation is required between the geotechnical and the structural engineer when designing this type of structure. A viaduct similar [4] to the one presented in this paper was design-checked by the author during his work as a senior structural engineer in Ireland.

3. Models description

Very often, it is impractical to model the entire structure with complex three-dimensional solid elements. A very complex numerical model can lead to inaccurate results than those predicted by simpler models, such as grillage or space frame. Due to the complex nonlinear nature of the soil behaviour under its loads, the analysis was limited to simple assumption that the mechanical parameters of the soil strictly follows only Hooke's law. In addition, it was assumed that the pressure under the footing foundation is lower than the soil bearing capacity. This is usually the case with a typical bridge foundation design. For the purpose of the analysis three models were built in the Abaqus FEA software [13]. The first complex model A3D, consists of three-dimensional solid elements representing the subgrade beneath the structure and the concrete footing foundation. In this model, the concrete pier support represents two-dimensional beam elements. The second L2D and the third H2D simple model consist of beam elements representing only the concrete pier support. The last two models represent an engineering approach to the design of this type of structure. The missing

elements from the complex model were replaced with vertical, horizontal, and rocking springs representing a rigid rectangular footing foundation resting on an elastic half-space. Equations which approximate foundation stiffnesses for a rigid rectangular footing resting on an elastic half-space can be obtained from references [8] and [10]. For the purposes of these analyses, the equations from reference [8] were used to calculate the foundation stiffnesses in the second model and from reference [10] to calculate the foundation stiffnesses in the third model. The equations for calculating the spring constants used in the analyses were derived by Russian scientists Doctor Dominik D. Barkan [11] and Profesor M.I. Gorbunov–Possadov [12]. An extensive number of field tests on a variety of soils and plates surfaces verified the validity of the spring constant coefficients used in these equations. Both models are shown in Fig. 1 and Fig. 2. Middle range value of Young's modulus for sand and gravel was used in all models, (Table 1). In the first model it is assumed that the subgrade beneath the structure in the form of a block of soil has a constant, uniform depth up to 19.2 m below the footing foundation. In all models a horizontal displacement in the Y direction of value 20 mm and a vertical force of value 18200 kN were applied to the top of the pier support. The horizontal displacement at the top of the pier support was caused by the thermal longitudinal expansion of the six-span viaduct deck and the braking force. The vertical force was caused by the dead, superimposed and live loads acting on the viaduct deck. The dead load of the pier support was also applied. In all models, the additional dead loads of the footing foundation and the subgrade were not included due to the absence of this structural element in the second and third model. The vertical force and displacement at the top of the pier support were taken from design calculation sheets of a similar structure, which was design-checked by the author. In the design-check of this viaduct, all loads were assumed in accordance with the standards [15] and [16]. Addition rotation of the top of the pier support around the direction of the X and Y axis were blocked only for clarity of this analyses. It should be emphasized that dead, superimposed and live loads, temperature variation across the deck, supports settlement and all stages of construction will cause rotation of the deck and pier support. This rotation will generate an additional spectrum of internal forces throughout the structure, which must be included in the structure design. All other boundary conditions at the top of the pier were released. The pier support is represented by Euler-Bernoulli 2-node cubic beams, type B33. In the first model, a kinematic type coupling was used to connect the beam elements with the solid elements representing the footing foundation. In this connection the bottom node of the beam element was the control point and the top surface region of the footing foundation directly under the pier support was the constraint region. The footing foundation represents 3072 general purpose 8-node linear brick elements type C3D8R with reduced integration and hourglass control. The same element type was used to build the block of subgrade beneath the footing foundation. The total number of elements representing the subgrade beneath the footing is equal to 262144. The interlayer interaction between the bottom surface of the footing foundation and the top surface of the subgrade beneath the footing was modelled as a standard contact surface-to-surface type discretization method with a finite sliding formulation. The contact interaction properties are a tangential behaviour with a static friction coefficient equal to 0.84. Additionally, normal behaviour with "Hard"

contact pressure overclosure and allowable separation after contact was applied. The adopted contact method permits some relative motion of the contact surfaces. The value of the static friction coefficient was calculated based on the internal friction angle of 40 degrees of dense sand and gravel obtained from reference [10]. The values of Young's modulus and Poisson's ratio of the materials selected for the analysis were taken from references [10, 14] and they are presented in Table 1.

Table 1. Models and material properties

Model	L2D160, (H2D160)	A3D
Subgrade	Dense sand and gravel	
E [MN/m^2]	160 (Middle range value)	
ν	0.3	
G [MN/m^2]	62	
L [m]	4.8	
B [m]	9.6	
β_φ (L/B)	0.46 (0.42)	
β_y (L/B)	1.03 (1.0)	
β_z (L/B)	2.15 (2.5)	
k_φ [MN/m/rad]	8954 (8102)	
k_y [MN/m]	1119 (1086)	
k_z [MN/m]	1283 (1492)	
Footing & pier	Concrete C50/60	
E_{cm} [MN/m^2]	37000	
ν	0.2	

where: L – length of the foundation (in plane of rotation for case of rocking), B – width of the foundation (along axis of rotation for case of rocking), E – subgrade Young's modulus, ν – Poisson's ratio, G – subgrade shear modulus, $(\beta_\varphi, \beta_\psi, \beta_z)$ – spring constant's coefficients for rectangular foundation, [8] and [10], (k_φ, k_y, k_z) – spring constants, [8] and [10]

The dimensions of the footing foundation and the subgrade block beneath the footing are shown in Fig. 1 and Fig. 3. Each vertical surface of the subgrade block has only a horizontal restraint applied perpendicularly to each surface. The bottom surface of this block has only a vertical restraint applied perpendicularly to this surface. In addition, it was assumed that the footing foundation is not backfilled. This situation may occur during temporary works in the vicinity of the footing foundation.

The equations for calculating the vertical and rocking stiffnesses presented in Table 2 were derived for a rigid rectangular footing foundation that rests on the surface of the elastic half-space.

Table 2. Equations for spring constants for rigid rectangular footing [8] and [10]

Shear modulus	(3.1) $G = \dfrac{E}{2\,(1+\nu)}$	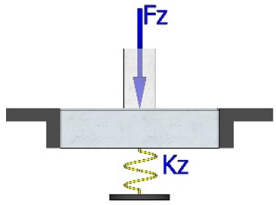
Vertical stiffness	(3.2) $k_z = \dfrac{G}{(1-\nu)}\beta_z\sqrt{BL}$	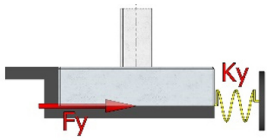
Horizontal stiffness	(3.3) $k_y = 2\,(1+\nu)\,G\beta_y\sqrt{BL}$	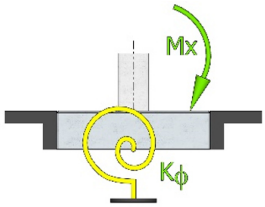
Rocking stiffness	(3.4) $k_\varphi = \dfrac{G}{(1-\nu)}\beta_\varphi BL^2$	

The formula to calculate the horizontal stiffness was derived based on the assumption of uniform distribution of the shear stress on the contact area and the calculations of the average horizontal displacement of this area [9]. In reference [8] the spring constants' coefficients for a rigid rectangular footing foundation depends on the ratio of the L/B of the footing foundation dimensions (Fig. 4).

The values of these coefficients are shown in Table 1. In reference [10] the spring constants' coefficients are constant values regardless of the size of the footing foundation. The values of the coefficients and the spring constants calculated on their basis are shown in brackets in Table 1. The impact of these parameters on the values and distribution of displacements and internal forces in the pier support is described in the next section.

4. Bending moment

Three numerical models of the pier support were analysed. The bending moment values from the complex model were compared with values from two simple models. Only the bending moment around the X axis was used in the analysis. The graph presenting the distribution of the bending moment M_x in the pier support for all models is shown in Fig. 5.

The results of static calculation show that the values ??of the bending moment M_x in the pier support are higher in each simple model L2D and H2D than in the complex model

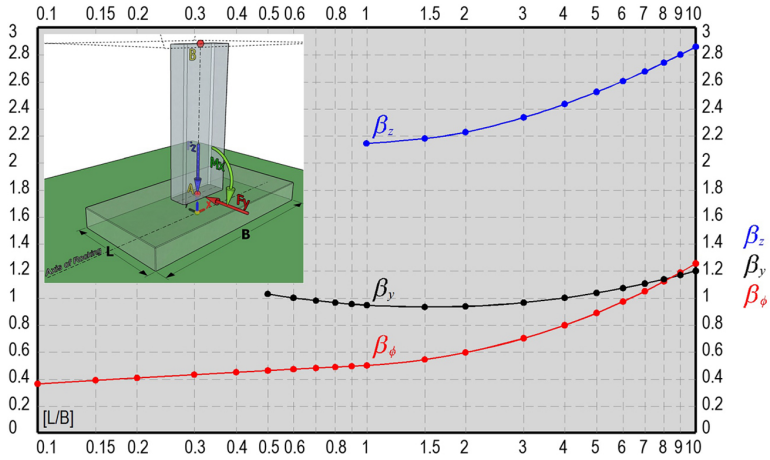

Fig. 4. Spring constant coefficients for rectangular foundation [8]

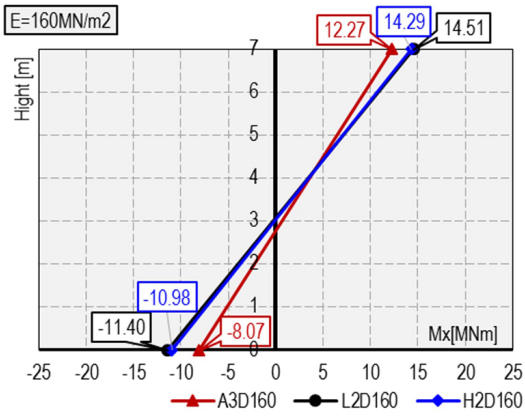

Fig. 5. Values and distribution of bending moments in the pier support

A3D. At the top of the pier support, the bending moment is about 16% to 18% higher in the simple models than in the complex model. At the bottom of the pier support, the bending moment is about 36% to 41% higher in the simple models than in the complex model. The analysis shows that the simple models generate higher values of bending moments compared to the complex three-dimensional model.

5. Shear force

The graph presenting the distribution of shear force T_y in the pier support for all models is shown in Fig. 6.

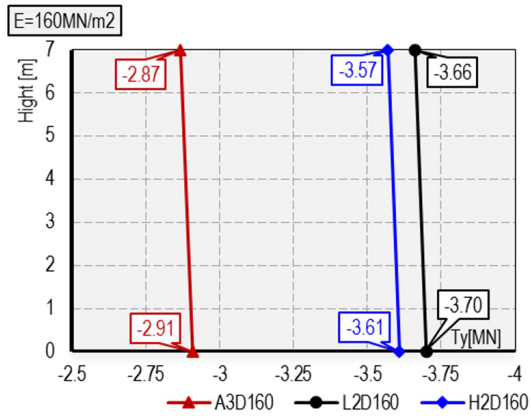

Fig. 6. Values and distribution of shear forces in the pier support

The results of static calculation show that the values ??of the shear force T_y in the pier support are higher in each simple model L2D and H2D than in the complex model A3D. At the top and bottom of the pier support, the shear forces are about 24% to 27% higher in the simple models than in the complex model. The analysis shows that the simple models generate higher values of shear force compared to the complex three-dimensional model.

6. Horizontal and vertical displacement

The graphs showing the displacements of the pier support in all models are shown in Fig. 7 and Fig. 8.

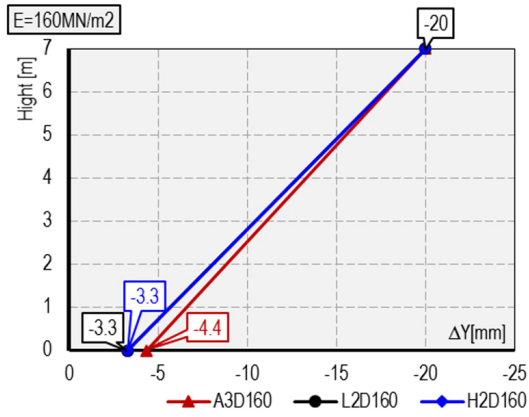

Fig. 7. Horizontal displacement, along the Y axis direction of the pier support

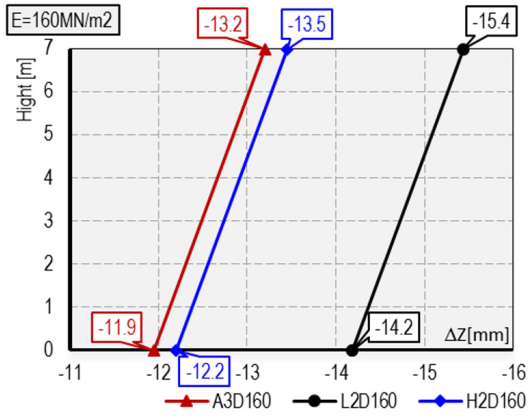

Fig. 8. Vertical displacement, along the Z-axis direction of the pier support

The horizontal displacements in the simple models L2D and H2D are smaller by approximately 1 mm compared to the complex model A3D. The vertical displacements in the simple models are larger by approximately 2 mm compared to the complex model. The analysis shows that the horizontal displacements are smaller and the vertical displacements are larger in the simple models than in the complex model.

7. Conclusions

The paper presents three methods of modelling of foundation stiffness beneath intermediate support of a 178 m long integral box girder viaduct and its impact on the values and distribution of displacements and internal forces in the pier of this support. Static calculations for all models were performed in the Abaqus FEA software [13]. The first complex model A3D, was built with three-dimensional solid elements representing the subgrade beneath the structure and the concrete footing foundation with two-dimensional beam elements representing the concrete pier support. The second L2D and the third H2D simple models were built with beam elements that represent only the concrete pier support. The missing elements from the complex model were replaced with vertical, horizontal, and rocking springs representing a rigid rectangular footing foundation resting on an elastic half-space. The equations for calculating the springs stiffness for a rigid rectangular footing given by Barkan [11] and Gorbunov–Possadov [12], used in the analyses, were derived from the theory for an elastic half space. Since the 1960s, these equations have been used in the design of concrete foundations for heavy industrial machinery that induces additional dynamic loads [11]. These equations are also used in the design of integral bridges [10].

The analysis shows that the internal forces in the pier support, such as the bending moment M_x and the shear force T_y, with the vertical displacement in the simple models L2D and H2D, have higher values than in the complex model A3D. The opposite is true for the horizontal displacement, which is lower in the simple models L2D and H2D than in

the complex model A3D. The variations in the results obtained from the static calculations are due to the different assumptions made in the numerical models. Despite the differences in the build of the complex model A3D and the last two simple models L2D and H2D, the displacement values of the pier support in all models are very similar. Higher internal forces in the simple models L2D and H2D will affect the amount of reinforcement or the necessity to upgrade the class of concrete in the pier support. In the case of complex ground conditions under the designed structure with complex loads acting on the structure, it is advisable to build a model consisting of three-dimensional elements that better reflects the current complex conditions. It should be emphasized that prior to design calculations that take subgrade stiffness into account the proper soil parameters for both the subgrade and the backfill must be determined. On the basis of such data the designer can build a numerical model of the structure founded on the specific subgrade stiffness. Therefore, close cooperation is required between the geotechnical and the structural engineer when designing integral viaducts.

Acknowledgements

Calculations have been carried out using resources provided by Wrocław Center for Networking and Supercomputing (https://wcss.pl), grant No. 554.

References

[1] A. Helowicz, "Wiadukty zintegrowane jednoprzęsłowe z prefabrykowanych dźwigarów sprężonych", presented at The 61 Scientific Conference, Bydgoszcz-Krynica Zdrój, Poland, Sep. 2015.

[2] A. Helowicz, "Mosty zintegrowane z prefabrykowanych dźwigarów sprężonych – doświadczenie projektanta", presented at The Scientific and Technical Conference Prestressed and Post-tension Concrete Structures, Kraków, Poland, 16-17 April, 2015.

[3] A. Helowicz, "Mostowe obiekty systemu Matière – doświadczenia projektanta", presented at The 62 Scientific Conference – Bydgoszcz–Krynica Zdrój, Sep. 2016.

[4] A. Helowicz, "Wieloprzęsłowe wiadukty zintegrowane z przęsłami skrzynkowymi – doświadczenie projektanta", *Acta Scientiarum Polonorum. Architectura*, vol. 16, no. 3, pp. 107–117, 2017. [Online]. Available: https://www.architectura.actapol.net/tom16/zeszyt3/16_3_107.pdf. [Accessed: 01. Aug. 2023].

[5] A. Helowicz, "Designing of small integral bridges and culverts – Designer experience", presented at The 65 Scientific Conference – Bydgoszcz-Krynica Zdrój, Sep. 2019.

[6] A. Helowicz, "Integral bridge and culvert design, Designer's experience", *Open Engineering,* vol. 10, no. 1, 2020, doi: 10.1515/eng-2020-0059.

[7] A. Helowicz, "Impact of subgrade and backfill stiffness on values and distribution of bending moments in integral box bridge", *Studia Geotechnica et Mechanica*, vol. 43, no. 2, pp. 90–98, doi: 10.2478/sgem-2021-0001.

[8] T.W. Lambe and R.V. Whitman, *Soil mechanics*. New York, USA: John Wiley, 1969.

[9] F.E. Richart, J.R. Hall, and R.D. Woods, *Vibrations of soils and foundations*. New Jersey, USA: Prentice-Hall, 1970.

[10] E.C. Hambly, *Bridge deck behaviour*, 2nd ed., London and New York: E & FN Spon, 1991.

[11] D.D. Barkan, *Dynamic of bases and foundation*. New York, USA: McGraw-Hill Book Company, 1962.

[12] M.I. Gorbunov–Possadov and R.V. Serebrjanyi, "Design of structures on elastic foundations", presented at The 5th International Conference on Soil Mechanics and Foundation Engineering, Paris, France, 1961.

[13] Abaqus FEA Software, “Abaqus analysis user’s manual”, Version 2016, Dassault Systemes. [Online]. Available: http://130.149.89.49:2080/v2016/index.html. [Accessed: 01. Aug. 2023].

[14] PN-EN 1992-1-1 Projektowanie konstrukcji z betonu. Część 1–1: Reguły ogólne i reguły dla budynków. PKN, 2008.

[15] BA42/96: 2003 The Design of Integral Bridges. Design Manual for Roads and Bridges, Vol. 1, Section 3, Part 12. London, UK: The Stationery Office, 2003.

[16] BD37/01: 2001 Loads for Highway Bridges. Design Manual for Roads and Bridges, Vol. 1, Section 3, Part 14. London, UK: The Stationery Office, 2001.

Modelowanie sztywności podłoża gruntowego pod podporą pośrednią wiaduktu zintegrowanego o długości 178 m

Słowa kluczowe: projekt, wiadukt zintegrowany, podpora pośrednia, filar, sztywność podłoża

Streszczenie:

W artykule przedstawiono trzy metody modelowania sztywności podłoża gruntowego pod podporą pośrednią wiaduktu zintegrowanego i analizę wpływu sposobu modelowania na wartości i rozkład przemieszczeń oraz sił wewnętrznych w filarze tej podpory. Wiadukt zintegrowany zdefiniować można, jako wiadukt, którego przęsło jest monolitycznie połączone z podporami pośrednimi i ścianami przyczółków i którego konstrukcja, w skutek oddziaływań termicznych i obciążeń zmiennych od ruchu pojazdów i pieszych, współpracuje z otaczającym ją gruntem. Obiekt taki nie wymaga zastosowania łożysk mostowych i prawie nigdy dylatacji mechanicznych lub płyt przejściowych. Prowadzi to do oszczędności finansowych przy ich budowie i ich eksploatacji. W analizie dotyczącej wpływu sposobu modelowania podłoża gruntowego pod podporą pośrednią założono, że filar i stopa fundamentowa zbudowane są z betonu zbrojonego klasy C50/60. Wartość modułu Younga wynoszącą 37 GPa i współczynnika Poissona 0,2 dla betonu przyjęto według Eurokodu 2. Analizowany filar jest monolitycznie połączony ze stopą fundamentową i przęsłem wiaduktu o przekroju skrzynkowym. Filar posadowiony jest bezpośrednio na gruncie i jest on ostatnim z pięciu podpór pośrednich przenoszących sześcioprzęsłowy wiadukt zintegrowany o długości 178 m. W analizie założono, że konstrukcja wiaduktu współpracuje z otaczającym go gruntem na skutek efektów termicznych i różnych obciążeń stałych i zmiennych. W rozpatrywanych modelach podłożem gruntowym jest zagęszczony piasek i żwir. Z literatury przyjęto średnią wartość modułu Younga dla tego materiału. Należy podkreślić, że przed przystąpieniem do projektowania konstrukcji współpracującej z otaczającym ją gruntem konieczne jest wcześniejsze określenie rzeczywistych parametrów fizycznych tego gruntu. Jest to możliwe jedynie na postawie badań geotechnicznych. Z tego względu przy projektowaniu wiaduktów zintegrowanych wymagana jest ścisła współpraca pomiędzy inżynierem geotechnikiem i projektantem konstrukcji. W programie Abaqus FEA zbudowano trzy modele numeryczne. Pierwszy model A3D pokazany na rysunku 1 przedstawia złożony model trójwymiarowy. Modele drugi L2D i trzeci H2D filara przedstawione na rysunku 2 pokazują uproszczone modele dwuwymiarowe. Sztywność podłoża i stopy fundamentowej w tych dwóch ostatnich modelach zastąpiono trzema więziami sprężystymi. Sztywność więzi sprężystej na obrót, na kierunku pionowym i na kierunku poziomym obliczono na podstawie równań podanych w publikacji [8] dla modelu L2D i publikacji [10] dla modelu H2D. Równania do obliczenia więzi sprężystych dla sztywnej prostokątnej stopy fundamentowej podane przez Barkana i Gorbunov–Possadov wyprowadzono z teorii sprężystości dla półprzestrzeni sprężystej. Od lat sześćdziesiątych ubiegłego wieku równania te znalazły zastosowanie przy projektowaniu fundamentów betonowych pod ciężkie maszyny przemysłowe wzbudzające dodatkowo obciążenia

dynamiczne. Równania te wykorzystuje się również przy projektowaniu mostów zintegrowanych [10]. We wszystkich modelach w górnej części filara przyłożono poziome przemieszczenie na kierunku osi Y o wartości 20 mm i siłę pionową na kierunku osi Z o wartości 18200 kN. Przemieszczenie górnej części filara spowodowane było termicznym wydłużeniem się sześcioprzęsłowego przęsła wiaduktu oraz siłą hamowania. Siła pionowa spowodowana była przez obciążenia stałe i zmienne działające na przęsło wiaduktu. We wszystkich modelach dodatkowo przyłożono ciężar własny filara. Natomiast, ze względu na brak w modelu drugim i trzecim elementów takich jak stopa fundamentowa i pod nią podłoża gruntowego w analizowanych modelach nie uwzględniono dodatkowego obciążenia od ciężaru własnego tych elementów. Przyłożone w analizowanych modelach przemieszczenie poziome i siłę pionową w górnej części filara wzięto z arkuszy obliczeniowych podobnej konstrukcji, której cały projekt wykonawczy był sprawdzany przez autora. Przy sprawdzeniu projektu podobnej konstrukcji wiaduktu wykorzystano normy brytyjskie. Dla przejrzystości wykonanej analizy we wszystkich modelach zablokowano obrót górnej części filara względem osi X i Y. Należy podkreślić, że obciążenia takie jak; ciężar własny konstrukcji i jej wyposażania, zmienność wiatru i temperatury, nierówne osiadanie podpór i wszystkie etapy wznoszenia konstrukcji wiaduktu spowodują przemieszczenia przęsła i filara. Przemieszczenia te wygenerują dodatkowe spektrum sił wewnętrznych w całej konstrukcji, które należy uwzględnić w projekcie konstrukcji wiaduktu. Wszystkie inne warunki brzegowe na górze filara zostały zwolnione. Ostatecznie wyniki obliczeń statycznych z modelu złożonego porównano z wynikami obliczeń statycznych uzyskanymi dla modeli prostych. W analizie dotyczącej wpływu sposobu modelowania podłoża gruntowego pod podporą pośrednią wykorzystano przemieszczenia pionowe na kierunku osi Z i poziome na kierunku osi Y oraz moment zginający M_x i siłę tnącą T_y w filarze. Autor pracy był projektantem sprawdzającym podobnej konstrukcji wiaduktu, który opisano w pracy zatytułowanej: “Wieloprzęsłowe wiadukty zintegrowane z przęsłami skrzynkowymi – doświadczenie projektanta”.

Received: 2023-08-06, Revised: 2023-09-12